DR. RUTH E ROSENSTEIN (Orcid ID : 0000-0002-8804-4395)

Article type : Original Article

INVOLVEMENT OF MICROGLIA IN EARLY AXOGLIAL ALTERATIONS OF THE OPTIC NERVE INDUCED BY EXPERIMENTAL GLAUCOMA

Melina P. Bordone[1], María F. González Fleitas[1], Laura A. Pasquini[2], Alejandra Bosco[3], Pablo H. Sande[1], Ruth E. Rosenstein[1]*, Damián Dorfman[1]*

1. Laboratory of Retinal Neurochemistry and Experimental Ophthalmology, Department of Human Biochemistry, School of Medicine/CEFyBO, University of Buenos Aires/CONICET, Paraguay 2155, 5th floor, Buenos Aires, Argentina. 2. Department of Biological Chemistry and Institute of Chemistry and Biological Physicochemistry, IQUIFIB, School of Pharmacy and Biochemistry, University of Buenos Aires, CONICET. 3. Department of Neurobiology and Anatomy, University of Utah, Salt Lake City, Presidents Circle Room 201 SLC, 84112, Utah, USA. *Both authors contributed equally to this work.

Corresponding author: Dr. Ruth E. Rosenstein,
Departamento de Bioquímica Humana,
Facultad de Medicina/CEFyBO
Universidad de Buenos Aires/CONICET
Paraguay 2155, 5°P, (1121),
Buenos Aires, ARGENTINA,
phone n°: 54-11-4508-3672 (ext. 37),
FAX n°: 54-11-4508-3672 (ext. 31),
e-mail: ruthr@fmed.uba.ar

This article has been accepted for publication and undergone full peer review but has not been through the copyediting, typesetting, pagination and proofreading process, which may lead to differences between this version and the Version of Record. Please cite this article as doi: 10.1111/jnc.14070

This article is protected by copyright. All rights reserved.

Accepted Article

Accepted Article

Running title: Microglia involvement in early glaucoma

Key Words: glaucoma; optic nerve; axoglial alterations; microglia

Abbreviations: CS, chondroitin sulfate; CTB, cholera toxin β-subunit; GFAP, glial fibrillary acidic protein; IOP, intraocular pressure; Iba-1, ionized calcium binding adaptor molecule 1; LGN, lateral geniculate nucleus; LFB, luxol fast blue; MINO, minocycline; MBP, myelin basic protein; ON, optic nerve; ONH, optic nerve head; pNFH, phosphorylated neurofilament heavy chain; RGC, retinal ganglion cell; SC, superior colliculus; SS, saline solution.

ABSTRACT

Glaucoma is a leading cause of blindness, characterized by retinal ganglion cell (RGC) loss and optic nerve (ON) damage. Cumulative evidence suggests glial cell involvement in the degeneration of the ON and RGCs. We analyzed the contribution of microglial reactivity to early axoglial alterations of the ON in an induced model of ocular hypertension. For this purpose, vehicle or chondroitin sulfate (CS) were weekly injected into the eye anterior chamber from *Wistar* rats for different intervals. The amount of Brn3a(+) RGC significantly decreased in CS-injected eyes for 10 and 15 (but not 6) weeks. A reduction in anterograde transport of β-subunit cholera toxin (CTB) was observed in the superior colliculus and the lateral geniculate nucleus contralateral to CS-injected eyes for 6 and 15 weeks. A disruption of CTB transport was observed at the proximal myelinated ON. A significant decrease in phosphorylated neurofilament heavy chain (pNFH)-immunoreactivity, an increase in Iba-1(+), ED1(+) (microglial markers), and glial fibrillary acidic protein (GFAP, astrocytes) (+) area, and decreased luxol fast blue (LFB) staining were observed in the ON at 6 and 15 weeks of ocular hypertension. Microglial reactivity involvement was examined through a daily treatment with minocycline (30 mg/kg, i.p.) for 2 weeks, after 4 weeks of ocular hypertension. Minocycline prevented the increase in

This article is protected by copyright. All rights reserved.

Accepted Article

Iba-1(+), ED-1(+), and GFAP(+) area, the decrease in pNFH-immunoreactivity and LFB staining, and the deficit in anterograde transport induced by 6 weeks of ocular hypertension. Thus, targeting microglial reactivity might prevent early axoglial alterations in the glaucomatous ON.

INTRODUCTION

Glaucoma, a leading cause of blindness, is a progressive optic neuropathy characterized by specific visual field defects associated with the loss of retinal ganglion cells (RGCs) and damage to the optic nerve head (ONH) (Quigley, 2011). Increased intraocular pressure (IOP) is the most accepted risk factor for developing glaucomatous neuropathy. In fact, current therapy in glaucoma is focused on decreasing IOP by pharmacological or surgical means, or with laser treatment. However, despite successful IOP control, many patients continue to lose vision (Musch et al., 2009), and it is becoming increasingly clear that the exclusive focus on IOP is not sufficient. To develop new treatments, it is necessary to have a better understanding of the mechanisms that lead to glaucomatous neuropathy. Considering the limitations of working with humans, animal models are a key tool for understanding pathogenic mechanisms of glaucoma. Several groups have established different models of glaucoma in rats (reviewed by Ishikawa et al., 2015), all of which have both advantages and disadvantages. We have developed an experimental model of glaucoma in rats through weekly injections of chondroitin sulfate (CS) in the eye anterior chamber (Belforte et al., 2010). Acute or chronic injections of CS significantly increase IOP as compared with vehicle-injected eye. Moreover, a significant decrease in flash visual evoked potentials was found in eyes receiving CS for 6 and 10 weeks, and a significant RGC and optic nerve (ON) axon loss was demonstrated in eyes injected with CS for 10 weeks, supporting the contention that intracameral injections of CS reproduce central characteristics of human primary open-angle glaucoma (Belforte et al., 2010).

This article is protected by copyright. All rights reserved.

Accepted Article

The degeneration of RGC soma that leads to glaucomatous vision loss has been attributed to an initial injury to axons within the ONH (Burgoyne et al., 1995; Chidlow et al., 2011; Howell et al., 2007; Morrison et al., 2011, Soto et al., 2008). In addition, defects in axonal transport have been reported as one of the earliest alterations in glaucoma (reviewed by Calkins, 2012). In that sense, progressive decline of anterograde axonal transport function (Crish et al., 2010), and retrograde transport deficits (Buckingham et al., 2008; Jakobs et al., 2005), preceding ON axon loss have been reported in different animal models of glaucoma. Although axonal transport interruption was originally attributed to constriction of the ONH as RGC axons exit the eye (Pease et al., 2000; Quigley et al., 2000), more recent reports suggest subtler intra-axonal mechanisms (Crish et al., 2010; reviewed by Crish and Calkins, 2011). Moreover, several studies have demonstrated that the progressive degeneration of ON axons and RGCs in glaucoma is accompanied by significant changes of different retina and ON glial cell types (Bosco et al., 2011; 2015; Crish et al., 2010; Hernandez et al., 2000; Libby et al., 2005; Naskar et al., 2002; Neufeld and Liu, 2003; Nakazawa et al., 2006; Qu and Jakobs, 2013; Sappington et al., 2010; Schlamp et al., 2006; Sun and Jakobs, 2012; Yuan and Neufeld, 2001). Although the precise interaction among glial cells, neurons, and axons is still unknown, it is possible that glial cells, particularly microglia, become directly pathogenic to axons. In the DBA/2J mouse, an established model of inherited, age-related pigmentary glaucoma (Libby et al., 2005), microglial cells become activated prior to detectable RGC loss (Bosco et al., 2011; 2015). In the same experimental model, it has been shown that the extent of microglia activation at the ONH is proportional to the severity of ON degeneration (Bosco et al., 2015). Moreover, it was shown that a long-term treatment of DBA/2J mice with minocycline which suppresses early microglial activation, significantly improves neuronal retrograde tracing from the superior colliculus (SC), the main retinal synaptic target in rodents (Bosco et al., 2008). Furthermore, minocycline delays RGC death in an experimental model

This article is protected by copyright. All rights reserved.

Accepted Article

of glaucoma in rats (Levkovitch-Verbin et al., 2006). However, the involvement of microglial reactivity in the early anterograde transport deficit and axoglial alterations of the ON induced by experimental glaucoma has not been previously examined. In that context, the aim of the present report was to analyze the contribution of microglial reactivity on early axoglial alterations of the ON in a rat glaucoma model induced by CS.

MATERIALS AND METHODS

Animals

Male *Wistar* rats (average weight 250 ± 40 g) from our own colony derived from a stock supplied by Charles River Breeding Laboratories (Wilmington, MA, U.S.A.) were housed in a standard animal room with food and water *ad libitum* under controlled temperature (21º ± 2ºC) and humidity conditions. The room was lighted by fluorescent lights that were turned on (at 8.00 A.M) and off (at 8.00 P.M.) automatically every 12 hours. All animal procedures were performed in strict accordance with the National Institutes of Health guide for the care and use of Laboratory animals. Rats were anesthetized with an intraperitoneal injection of ketamine hydrochloride (50 mg/kg) and xylazine hydrochloride (7 mg/kg). A total number of 85 rats were used for the experiments, distributed as follows: 15 animals for Brn3a quantification, 30 animals for CTB detection (including minocycline-treated rats), 20 animals for luxol fast blue experiments, and 20 animals for immunohistochemistry experiments (including minocycline-treated animals). The experimental procedures reported here were approved by the Animal Care Committee of the Center for Pharmacological and Botanical Studies, National Research Council, and by the Institutional Committee for the Care and Use of Laboratory Animals (CICUAL) from the School of Medicine, University of Buenos Aires. Animals were identified by earmark numbers, and the randomizing protocol was performed by assigning them to each treatment, using a random number generator (http://www.randomizer.org/form.htm)

This article is protected by copyright. All rights reserved.

Accepted Article

Experimental model of glaucoma

Weekly injections of CS were performed as previously described (Belforte et al., 2010). Briefly, under a surgical microscope (OMNI MDU XY, Carl Zeiss, USA) 20 µl of 40% CS (Sigma Chemical Co., St. Louis, MO, USA, catalog # C9819) in saline solution were injected into one eye instilled with 0.5% proparacaine hydrochloride, using a Hamilton syringe with a 30G needle, while the same volume of vehicle was injected in the contralateral eye. The content of the syringe was slowly and progressively injected to avoid ocular ischemia and lens damage. Rats that developed cataract or *phtisis bulbi* (4 animals) were excluded from the experiments.

IOP assessment

IOP was assessed each week, as previously described (Belforte et al., 2010). Briefly, animals were wrapped in a small towel, and IOP readings were obtained with a TonoPen XL (Mentor, Norwell, MA, USA) contacting firmly the cornea. TonoPen readings differed less than 10% (standard error). The mean of these readings was recorded as the IOP for each eye. Mean values from each rat were averaged, and the resultant mean value was used to compute the group mean IOP ± SE. IOP determinations were performed between 11.00 and 12.00 h to correct for diurnal variations in this parameter (Moreno et al., 2005).

Cholera toxin β-subunit transport studies

Animals were anesthetized, and a drop of proparacaine (0.5%, Anestalcon, Alcon Laboratories, Buenos Aires, Argentina) was topically administered for local anaesthesia. Four µl of 0.1% cholera toxin β-subunit (CTB) conjugated to Alexa 488 (cat. #: c22841, Molecular Probes Inc., Eugene, OR, USA) in sterile saline solution were injected into the vitreous, using a 30G Hamilton syringe (Hamilton, Reno, NV, USA), as previously reported (Dorfman et al., 2013). The injections were applied 1 mm from the limbus, and the needle was left in the eye for 30 s to prevent volume loss. At

This article is protected by copyright. All rights reserved.

Accepted Article

three days post-injection, rats were anesthetized and intracardially perfused with 4% paraformaldehyde in phosphate buffer (PBS), pH 7.4. Brains were carefully removed, post-fixed overnight at 4°C, cryoprotected in sucrose solutions (10, 20, and 30%), and embedded in OCT compound (Crioplast®, Biopack, Buenos Aires, Argentina). Coronal sections (40 µm) were obtained at the level of lateral geniculate nucleus (LGN) and SC using a freezing microtome CM 1850 (Leica, Germany) and observed under an epifluorescence microscope (BX50, Olympus, Duarte, CA, USA). Additionally, to determine the site of transport disruption, eyeballs together with 2 mm of the ON were carefully dissected and processed similarly to brains, with the cornea and lens removed before cryoprotecting the eye in a sucrose gradient. In order to obtain longitudinal ON sections and transverse retinal sections, eyecups were sagittally sectioned at the level of the ONH (15 µm thickness) and mounted in superfrost microscope slides (Erie Scientific Company, Portsmouth, New Hampshire, USA).

Histological evaluation of the ON

Deeply anesthetized animals were intracardially perfused with saline solution, followed by 4% paraformaldehyde in PBS (pH 7.4). Eyes and ON samples from the ONH near the optic chiasm were obtained and post-fixed for 24 h in the same fixative solution at 4ºC. After several washes, the samples were dehydrated, cleared in n-butanol and embedded in paraffin wax. Serial transverse sections (5 µm) of the myelinated proximal ON were obtained using a microtome (Leica, Leica Microsystems, Buenos Aires, Argentina).

Immunohistochemical studies

The following antibodies were used: a goat anti-Brn3a (AB Registry ID: AB_2167511, 1:500; Santa Cruz Biotechnology, Buenos Aires, Argentina), a mouse monoclonal anti-phosphorylated neurofilament heavy chain (pNFH) (AB Registry ID: AB_448147, 1:1000; Abcam Inc, Buenos Aires,

This article is protected by copyright. All rights reserved.

Argentina), a goat anti-ionized calcium binding adaptor molecule 1 (Iba-1) (AB Registry ID: AB_2224402, 1:500; Abcam Inc., Buenos Aires, Argentina), a mouse anti-ED1 (AB Registry ID: AB_1141557, 1:200; Abcam Inc., Buenos Aires, Argentina), a mouse monoclonal anti-glial fibrillary acidic protein (GFAP) conjugated to Cy3 (AB Registry ID: AB_476889, 1:1200; Sigma Chemical Co., St Louis, MO, USA), a rabbit polyclonal anti- myelin basic protein (MBP, 1:1000, kindly supplied by Dr. Campagnoni, Mental Retardation Research Center, University of California, Los Angeles, CA, USA), a donkey anti-goat secondary antibody conjugated to Alexa 568 (AB Registry ID: AB_2636995, 1:500; Life Technologies, USA), a goat anti-mouse and a donkey anti-mouse secondary antibodies conjugated to Alexa 488 (Cat. #: ab150105, 1:500; Molecular Probes, Buenos Aires, Argentina), and a donkey anti-rabbit secondary antibody conjugated to Alexa 568 (Cat# ab175470, 1:500; Molecular Probes, Buenos Aires, Argentina).

For ON immunohistochemical studies, proximal ON transversal sections were deparaffinised, hydrated and antigen retrieval was performed (except for MBP immunodetection) with citrate buffer (pH 6.3) for 30 min at 90°C. After permeabilization with 0.1% Triton X-100 in 0.1 mol/L PBS for 10 min, sections were unspecifically blocked with normal horse serum (2%) for 1 h, followed by incubation with primary antibodies overnight at 4°C. Then, samples were incubated with secondary antibodies for 2 h at room temperature, and mounted with fluorescent mounting medium (Dako, Glostrup, Denmark), and viewed at 200X magnification under a fluorescence microscope. To confirm specificity, primary antibodies were avoided in some sections.

For MBP immunodetection, longitudinal optic nerve cryostat sections were obtained and immersed in 5% normal horse serum, 0.3% Triton X-100 in 0.1M PBS for 2 h, for unspecific blockade and permeabilization, and then incubated overnight at 4°C with primary antibody diluted in 2% normal horse serum 0.1% Triton X-100 in 0.1 M PBS.

This article is protected by copyright. All rights reserved.

Accepted Article

For immunodetection of Brn3a, 15 µm thickness retinal sections were obtained using a freezing microtome, and mounted in superfrost microscope slides. For antigen retrieval, the same protocol described above was followed. All images were captured using identical exposure time, under an epifluorescence microscope (BX50; Olympus, Tokyo, Japan) connected to a video camera (3CCD; Sony, Tokyo, Japan), attached to a computer running image analysis software (Image-Pro Plus; Media Cybernetics Inc., Bethesda, MD, USA). Immunofluorescence studies were performed analyzing comparative digital images from different samples with the same brightness, and contrast settings.

Luxol fast blue staining

Deparaffinised transversal proximal ON sections were re-hydrated and incubated with 0.1 % luxol fast blue (LFB, Biopack, Buenos Aires, Argentina) in acidified 95% ethanol overnight at 60°C. Li_2CO_3 (0.01 %) for 5 min in 0.5 % neutral red (Biopack, Buenos Aires, Argentina) was used for differentiation and nuclei counterstaining. Sections were mounted and viewed under a light microscope (Nikon Eclipse E400, Tokyo, Japan). Light microscopic images (200X) were digitally captured via a Nikon Coolpix S10 camera (Nikon, Tokyo, Japan).

Morphometric Analysis

To adjust brightness and contrast, all images were assembled and processed using Adobe Photoshop CS4 (Adobe Systems, San Jose, CA, USA), with no other adjustments. For morphometric image processing and analysis, digitalized captured TIFF images were transferred to ImageJ software version 1.42q (National Institutes of Health, Bethesda, Maryland; http://imagej.nih.gov/ij/). For morphometric analysis of Brn3a(+) cell density, whole retinal microphotographs were obtained (×400) at 1 mm dorsal and ventral from the optic disk and Brn3a(+) RGC number/100 µm was assessed. For each eye, four different sections (i.e., one every 20 µm) were obtained where the ON exiting the eye was visible.

This article is protected by copyright. All rights reserved.

Accepted Article

Accepted Article

Results from these sections were averaged and used as the mean value. The mean of 5 retinas was used as the representative value for each group. In this way, only similar retinal eccentricities were analyzed in every group, avoiding introducing bias.

ON images at 200X magnification were processed to obtain 4 representative quadrants, 10,000 μm^2 each. The average immunopositive area of the four quadrants from each nerve was determined using Image J software. For LFB staining, the percentage of LFB per region was determined using the colour threshold tool (Image J software), to avoid neutral red staining. The mean of 5 ONs was recorded as the representative value for each group. Data were analyzed by treatment-blind operators.

Minocycline treatment

Animals injected with vehicle in one eye and CS in the contralateral eye were randomly divided in two groups: one treated with saline solution (SS), and one treated daily (i.p.) with 30 mg/kg minocycline (Sigma, Aldrich Corp, St Louis, MO, USA). Minocycline or saline treatment started at 4 weeks of intracameral injections and continued until 6 weeks of ocular hypertension (i.e., 2-week treatment). The manner of administration and dosage of minocycline were selected on the basis of a previous report (Guasti et al., 2009).

Statistical analysis

Experimenters were blinded to group assignment and outcome assessment for all animal experiments. Data are presented as mean ± standard error (SE). Statistical analysis of results was performed by two-way analysis of variance (ANOVA), followed by Tukey´s test. P values below 0.05 were considered statistically significant. Sample size calculation was performed using the statistical program Infostat (FCA, University of Cordoba, Cordoba, Argentina), and the power analysis ranged between 80 and 87% for all the studies.

This article is protected by copyright. All rights reserved.

Accepted Article

RESULTS

Table 1 summarizes the average IOP from eyes injected weekly with vehicle or CS for 3, 6, 10 or 15 weeks. IOP was significantly higher in CS- than in vehicle-injected eyes at all time points examined. No significant differences in IOP values were observed between naïve eyes and eyes injected with vehicle along the study (data not shown). In order to analyze the effect of CS-induced ocular hypertension on RGCs, Brn3a-immunoreactivity was assessed at several time points. A significant decrease in Brn3a(+) cell number was observed in the ganglion cell layer (GCL) from eyes injected with CS for 10 and 15 (but not 6) weeks, as shown in Figure 1.

The retinal anterograde transport to the SC and LGN in naïve animals and in animals in which one eye was hypertensive for 3, 6, or 15 weeks was analyzed using CTB. As shown in Figure 2A, CTB labeled the entire retinotopic projection to the *stratum zonale* and the *stratum griseum superficiale*, the most superficial layers of the SC, which received projections from naïve eyes. A similar profile was observed in the SC which received projections from vehicle- and CS-injected eyes for 3 weeks, whereas a reduction in CTB staining was observed in the SC which received projections from CS-injected eyes for 6 and 15 weeks of ocular hypertension. A similar profile of decrease in CTB labeling was observed in the LGN which received afferents from hypertensive eyes for 6 and 15 (but not 3) weeks (Figure 2B). A panoramic view of CTB staining in longitudinal sections obtained at the proximal portion of the ON from eyes injected with vehicle or CS for 6 weeks is shown in Figure 2C. In ONs from eyes that were hypertensive for 6 weeks, a disruption of CTB anterograde transport occurred at the ON proximal (at 0.4 - 0.6 mm from the retina) myelinated portion, as indicated by MBP-immunoreactivity localization in the ON from a naïve eye (Figure 2C).

To assess the effect of ocular hypertension on the ON structure, axons, microglia, astrocytes, and the myelination state were analyzed in transverse sections of the ON proximal portion. As shown in Figure 3, a significant decrease in pNFH-immunoreactivity was observed both at 6 and 15 weeks of

This article is protected by copyright. All rights reserved.

Accepted Article

ocular hypertension. No differences in pNFH(+) area were observed between ONs from eyes injected with vehicle for 6 and 15 weeks. Microglial cells were analyzed by Iba-1 and ED1-immunoreactivity (Figure 4). Measurement of Iba-1(+) area indicated a significant increase of this parameter at 6 weeks of CS treatment, which was lower (but still significantly higher than in control ONs) at 15 weeks of ocular hypertension. In the ON from vehicle-injected eyes, ED1-immunoreactivity was almost undetectable, whereas at 6 weeks of ocular hypertension, an increase in this parameter which progressed at 15 weeks of ocular hypertension was observed. Moreover, a significant increase in GFAP(+) area was found at 6 and 15 weeks of ocular hypertension in the proximal ON, as shown in Figure 5A. Myelin alterations were assessed by LFB staining. In the proximal portion of the ON, signs of demyelination were evident at 6 weeks of ocular hypertension which progressed at 15 weeks of treatment (Figure 5B). No differences in Iba-1-, ED1-, GFAP- and pNFH- immunoreactivity and LFB staining were observed between naïve and vehicle-injected eyes along the study (data not shown).

In order to analyze the involvement of microglial reactivity on ON alterations induced by ocular hypertension, saline solution (SS) or minocycline were daily administered (30 mg/kg, i.p.) for 2 weeks, starting at 4 weeks of intracameral injections of vehicle or CS. The treatment with minocycline did not affect IOP in eyes injected with vehicle or CS for 6 weeks (i.e., IOP (mmHg) was: vehicle + SS = 11.5 ± 0.9; vehicle + minocycline = 12.2 ± 0.8; CS + SS = 23.5 ± 0.9, and CS + minocycline = 22.8 ± 0.7), but it significantly prevented the increase in Iba-1(+) and ED-1(+) area induced by ocular hypertension (Figure 6). In addition, minocycline prevented an increase in GFAP immunoreactivity, as well as a decrease in LFB staining induced by ocular hypertension (Figure 7). Furthermore, the treatment with minocycline prevented the decrease in pNFH-immunoreactivity induced by ocular hypertension, and preserved CTB anterograde transport from the retina to the SC and LGN (Figure 8).

This article is protected by copyright. All rights reserved.

Accepted Article

DISCUSSION

The present results support the involvement of microglial reactivity on the early axoglial alterations in the proximal portion of the ON induced by experimental glaucoma in rats.

Using rodent models, new insights have been gained into glaucoma pathogenesis; however, a consistent understanding of the chronology of alterations in glaucoma is still to be reached. In this sense, it is still unclear whether axon pathology initiates or follows RGC loss during glaucoma. Whilst a body of evidence supports the former hypothesis (Buckingham et al., 2008, Howell et al., 2007; Calkins, 2012; Crish et al., 2010), other data endorse the view that atrophy of RGC soma occurs first (Soto et al., 2008). As shown herein, a deficit in CTB anterograde transport from the retina to the SC and LGN at 6 and 15 (but not 3) weeks of treatment with CS was observed. RGC unmyelinated axons converge at the ONH, where they exit the ocular globe and become the myelinated ON. In rats, most (~ 98%) fibers decussate at the optic chiasm, forming the contralateral optic tract, and synapsing in the LGN and SC (Kondo et al., 1993). CTB is a reliable tracer that has been extensively used to analyze the communication between the retina and its synaptic targets (Buckingham et al., 2008; Crish et al., 2010; Fernandez et al., 2012; Dorfman et al., 2013). A progressive deficit in the anterograde (Crish and Calkins, 2011; Dengler-Crish et al., 2014), and retrograde (Buckingham et al., 2008; Pease et al., 2000) axonal transport prior to neuronal loss was previously described in some experimental models of glaucoma, and it was more recently demonstrated that anterograde transport is affected earlier and to a larger degree than retrograde transport in glaucomatous DBA/2J mice (Dengler-Crish et al., 2014). The present results support that experimental glaucoma provoked an early “misconnection” between the retina and its central targets, which preceded RGC loss, and further support the axonal compartment as a specific site of early glaucomatous dysfunction. In the following experiments, we chose to wait 6 or 15 weeks of CS-induced ocular hypertension, in order to analyze pathological events at early (i.e., when anterograde transport is reduced without RGC loss), and late (i.e., after

This article is protected by copyright. All rights reserved.

Accepted Article

RGC loss) stages of experimental glaucoma. In order to identify the anterograde transport disruption locus along the ON in CS-induced glaucoma, intraorbital (unmyelinated and myelinated) ON sections labeled with CTB were analyzed. A disruption of CTB transport seemed to occur at the proximal, MBP(+) portion of the ON, beyond the ONH. Previous studies have shown that chronically elevated IOP disrupts retrograde axonal transport to the retina at ONH level (Chidlow et al., 2011; Martin et al., 2006). On the other hand, both in DBA/2J mice and in a rat model of glaucoma induced by microbeads, Crish et al. (2010) reported that CTB axonal transport dysfunction and axon degeneration appear first at the SC, with a distal-proximal progression, with ONH deficits occurring much later. Currently, we do not have any explanation for this discrepancy. However, differences in animal model, species and/or strains, as well as animal age (~ 8 months old DBA/2J mice, and ~ 7 months old *Brown Norway* rats in the report by Crish et al., (2010) and ~ 4 months old *Wistar* rats in our case) could account for this disagreement. In the inbred mouse strain DBA/2J, pigmentary glaucoma is caused by an early iris atrophy and pigment dispersion that block aqueous outflow (Libby et al., 2005), provoking ocular hypertension through a different mechanism and with a different time frame from those involved in CS-induced ocular hypertension (Belforte et al., 2010). On the other hand, although the treatment with microbeads induces IOP elevations of ~ 10 mm Hg in a similar “scenario” to that observed in CS-injected eyes, the influence of age in the former model is supported by the fact that CTB labeling in the SC was unaffected in *Brown Norway* rats, which received an injection of microbeads into the aqueous chamber (Crish et al., 2010) at a similar age to that of *Wistar* rats included in the present study. In line with this, an age-related susceptibility of the rat retina to increased IOP has been demonstrated (Tan et al., 2015). Experimental glaucoma induced by CS provoked a progressive deficit in CTB transport from the retina to the LGN (which lies anterior to the SC, i.e., more proximal to the eye), that was also diminished at an early stage of glaucoma. This result also contrasts the finding that the failure of CTB transport occurs first in the SC and then at more anterior sites in order of increasing proximity to the eye, as described by Crish et al. (2010), and

This article is protected by copyright. All rights reserved.

Accepted Article

supports the occurrence of a more proximal alteration in the anterograde transport, at least in the glaucoma model induced by CS. Interestingly, we have previously shown that experimental diabetes provokes early axoglial alterations in the distal (close to the chiasm) but not proximal ON portion (Fernandez et al., 2012), suggesting that the damage localization along the ON may show a insult type-dependent profile.

Neurofilament protein is one of the the main components of the neuron cytoskeleton, it mainly distributes in neuronal soma and processes, and participates in maintaining cell normal morphology (Sihag et al., 2007). In axons (including ON axons), almost all neurofilaments are phosphorylated, while these proteins are primarily dephosphorylated in the perikarya and dendrites (Leterrier et al., 1996). Phosphorylation of NFH seems to be a key mechanism in the formation of neurofilament crossbridges, and it is deeply involved in axonal transport, axonal plasticity, and neuronal morphology (Nixon and Sihag, 1991). A decrease in NFH phosphorylation was described in prelaminar, laminar, and proximal post-laminar regions in experimental models of glaucoma in mice (Son et al., 2010), and monkeys (Kashiwagi et al., 2003). Supporting this, a significant decrease in pNFH-immunoreactivity was observed in the proximal portion of the ON from eyes with 6 or 15 weeks of ocular hypertension, which suggest that changes to the axon cytoskeleton may be involved in the axonal transport deficit induced by chronic ocular hypertension.

Microglial cells are central nervous system resident innate immune cells, endowed with sensor and effector functions, as well as phagocytic capacity during physiological and pathological conditions (reviewed by Perry and Teeling, 2013; Streit et al., 2005). These cells respond to neuronal stress or injury by adopting an activated state, in which they progress to an activated phenotype (Lee et al., 2008; Tambuyzer et al., 2009) which includes alterations in cellular morphology, changes in the structure of the cellular processes, redistribution, migratory characteristics, expression of various

This article is protected by copyright. All rights reserved.

cytokines, proliferation, and phagocytic activity (Czirr and Wyss-Coray, 2012; Raivich and Banati, 2004). Reactive microglia were detected in the retina and ON from axotomized eyes (Garcia-Valenzuela et al., 2005; Sobrado-Calvo et al., 2007), and after ischemia/reperfusion injury (Davies et al., 2006). In human glaucoma, there is abnormal microglial reactivity and redistribution within the ONH (Neufeld, 1999; Yuan and Neufeld, 2001). Moreover, reactive microgliosis is detectable in retinas and ONs in animal models of glaucoma (Bosco et al., 2011; Naskar et al., 2002; Son et al., 2010). An increase in Iba-1- and ED1- immunoreactivity at the proximal ON was already evident at 6 weeks of ocular hypertension (ahead of RGC loss), supporting that microglial activation in the proximal portion of the ON may represent an early event in CS-induced experimental glaucoma. Supporting this, it was previously demonstrated that microglia become activated before RGC loss in unmyelinated and myelinated ON regions in other experimental models of glaucoma in mice (Bosco et al., 2011), and rats (Ebneter et al., 2010). Although Iba-1(+) and ED1(+) area significantly increased in the proximal ON from glaucomatous eyes, a different profile was observed for the levels of each of these markers, since Iba-1 levels decreased from 6 to 15 weeks of ocular hypertension, while ED1 showed a change in the opposite direction, which is in agreement with the fact that Iba-1 labels both quiescent and activated microglia (providing a microglial density index), whereas the antigen ED1 represents a measure of phagocytic activity (Ebneter et al., 2010). These results support a time of ocular hypertension-dependent progression of microglial reactivity in the proximal portion of the ON. However, since these immunohistochemical markers (Iba-1 and ED1) are also expressed in macrophages, the presence of this type of cells in the glaucomatous ON cannot be ruled out.

Besides microglial reactivity and axon alterations, astrocytosis is an index of many neurodegenerative conditions, including experimental (Son et al., 2010; Yang et al., 2013; Zhou et al., 2009), and human (Hernandez, 2000; Kerr et al., 2011) glaucoma. Supporting this, reactive astrogliosis (as indicated by

This article is protected by copyright. All rights reserved.

Accepted Article

Accepted Article

an increase in GFAP-immunoreactivity) was observed in the ON proximal portion from glaucomatous eyes at early stages (i.e., 6 weeks of ocular hypertension), that persisted at late (i.e., 15 weeks of treatment with CS) stages of the experimental disease.

Oligodendrocyte death in the ON preceding RGC loss has been shown in laser-induced ocular hypertension in mice (Nakazawa et al., 2006). Supporting this, at 6 weeks of CS- induced ocular hypertension, a slight (but significant) decrease in LFB staining, which progressed at 15 weeks of treatment, was observed. In contrast, in DBA/2J mouse and in a rat ocular hypertension model, Son et al., (2010) have shown a modest loss of oligodendrocytes that occurs after axons had already degenerated. Therefore, the early myelin alterations shown in some experimental models of glaucoma may not be generalized to others. In the CS-induced model of glaucoma, the early decrease in LFB staining was concomitant with a decrease in anterograde transport and pNFH-immunorectivity, astrocytosis and increased microglial reactivity. Thus, although we could not determine whether the early damage provoked by CS-induced glaucoma primarily affected axons or glial cells, our results suggest that the reciprocal communication between axons and glia in the proximal ON can be negatively regulated at early stages of the experimental disease.

Microglial reactivity is a common feature of neurological disorders. In order to analyze whether it contributes to neuronal and/or glial damage, we analyzed the effect of minocycline on early axoglial alterations of the proximal portion of the ON induced by ocular hypertension. Minocycline, which crosses the blood-brain barrier, is an inhibitor of microglial activation in the retina (Peng et al., 2014). Moreover, minocycline delays the death of axotomized RGCs by inhibiting microglia activation (Baptiste et al., 2005), and it reduces retinal microglia activation, and improves ON integrity in glaucomatous DBA/2J mice (Bosco et al., 2008). As expected, the treatment with minocycline significantly prevented the increase in Iba-1- and ED-1-immunoreactivity in the proximal portion of

This article is protected by copyright. All rights reserved.

Accepted Article

the ON from eyes that were hypertensive for 6 weeks. Moreover, a 2-week treatment with minocycline significantly prevented the decrease in pNFH- and the increase in GFAP-immunoreactivity, as well as the decrease in LFB staining. Suporting this, it was shown that inhibition of microglial activation with minocycline leads to a decrease of astrogliosis in mouse hippocampus induced by heat stress (Lee et al., 2015), and cuprizone-induced demyelination (Pasquini et al., 2007).

Concurrently with the structural preservation, minocycline also preserved the anterograde transport of CTB from the retina to the SC and LGN. Therefore, although a more detailed temporal course of proximal ON microglial reactivity (particularly, before and after 6 weeks of ocular hypertension) deserves to be analyzed, the present results support the involvement of microglial reactivity in axoglial alterations in the proximal portion of the ON and, in turn, in the misconnection between the retina and its synaptic targets induced by experimental glaucoma.

Axonal damage often results in axonal degeneration and permanent loss of the cell body. ON transection or crush induce a rapid stress response in RGCs that finally results in neuronal death (Quigley et al., 1995; You et al., 2012). Therefore, although in the present report, the effect of minocycline was assessed at early stages of glaucoma (before RGC loss), it seems likely that the axonal protection conferred by minocycline could account for its protective effect on RGCs demonstrated in other experimental models of glaucoma (Levkovitch-Verbin et al., 2006, 2014; Wang et al., 2014), and that the restoration of anterograde transport along RGC axons and the prevention of axoglial alterations in the proximal ON might be early therapeutic targets for glaucoma treatment.

This article is protected by copyright. All rights reserved.

Accepted Article

Conclusions

The significance of this observation, if confirmed in the human condition, supports the targeting of ON microglial reactivity to prevent early axoglial alterations in the proximal ON and consequently, to slow the progression of glaucoma.

```
Involves human subjects: No
If yes: Informed consent & ethics approval achieved:
=> if yes, please ensure that the info "Informed consent was achieved for all
subjects, and the experiments were approved by the local ethics committee." is
included in the Methods.
```

Acknowledgments

This research was supported by grants from the Agencia Nacional de Promoción Científica y Tecnológica; Consejo Nacional de Investigaciones Científicas y Técnicas; University of Buenos Aires; Argentina, and ARVO Foundation/Collaborative Research Fellowship. The funding organizations have no role in the design or conduct of this research. The authors report no conflicts of interest.

REFERENCES

Baptiste D., Powell K., Jollimore C., Hamilton C., LeVatte T., Archibald M., Chauhan B., Robertson G. and Kelly. M. (2005) Effects of minocycline and tetracycline on retinal ganglion cell survival after axotomy. Neuroscience 134, 575-582.

Belforte N., Sande P., de Zavalía N., Knepper P. A. and Rosenstein, R. E. (2010) Effect of chondroitin sulfate on intraocular pressure in rats. Invest. Ophthalmol. Vis. Sci. 51, 5768-5775.

Bosco A., Inman D. M., Steele M. R., Wu G., Soto I., Marsh-Armstrong N., Hubbard W. C., Calkins D. J., Horner P. J. and Vetter M.L. (2008) Reduced retina microglial activation and improved optic

This article is protected by copyright. All rights reserved.

nerve integrity with minocycline treatment in the DBA/2J mouse model of glaucoma. Invest. Ophthalmol. Vis. Sci. 49, 1437-1446.

Bosco, A., Steele M. R. and Vetter M. L. (2011) Early microglia activation in a mouse model of chronic glaucoma. J. Comp. Neurol. 519, 599-620.

Bosco A., Romero C. O., Breen K. T., Chagovetz, A. A., Steele M. R., Ambati B. K. and Vetter M. L. (2015) Neurodegeneration severity can be predicted from early microglia alterations monitored in vivo in a mouse model of chronic glaucoma. Dis. Model. Mech. 8, 443-455.

Buckingham B. P., Inman D. M., Lambert W., Oglesby E., Calkins D. J., Steele M. R., Vetter M. L., Marsh-Armstrong N. and Horner P. J. (2008) Progressive ganglion cell degeneration precedes neuronal loss in a mouse model of glaucoma. J. Neurosci. 28, 2735-2744.

Burgoyne C. F., Quigley H. A., Thompson H. W., Vitale S. and Varma R. (1995) Early changes in optic disc compliance and surface position in experimental glaucoma. Ophthalmology 102, 1800-1809.

Calkins D. J. (2012) Critical pathogenic events underlying progression of neurodegeneration in glaucoma. Prog. Retin. Eye Res. 31, 702-719.

Chidlow G., Ebneter A., Wood J. P. and Casson R. J. (2011) The optic nerve head is the site of axonal transport disruption, axonal cytoskeleton damage and putative axonal regeneration failure in a rat model of glaucoma. Acta Neuropathol. 121, 737-751.

Accepted Article

This article is protected by copyright. All rights reserved.

Accepted Article

Crish S. D. and Calkins D. J. (2011) Neurodegeneration in glaucoma: progression and calcium-dependent intracellular mechanisms. Neuroscience 176, 1-11.

Crish S. D., Sappington R. M., Inman D. M., Horner P. J. and Calkins D. J. (2010) Distal axonopathy with structural persistence in glaucomatous neurodegeneration. Proc. Natl. Acad. Sci. U.S.A 107, 5196-5201.

Czirr E. and Wyss-Coray T. (2012) The immunology of neurodegeneration. J. Clin. Invest. 122,1156-1163.

Davies M. H., Eubanks J. P. and Powers M. R. (2006) Microglia and macrophages are increased in response to ischemia-induced retinopathy in the mouse retina. Mol. Vis. 12, 467-477.

Dengler-Crish C. M., Smith M. A., Inman D. M., Wilson G. N., Young J. W. and Crish S. D. (2014) Anterograde transport blockade precedes deficits in retrograde transport in the visual projection of the DBA/2J mouse model of glaucoma. Front. Neurosci. 8, 290.

Dorfman D., Fernandez D. C., Chianelli M., Miranda M., Aranda M. L. and Rosenstein R. E. (2013) Post-ischemic environmental enrichment protects the retina from ischemic damage in adult rats. Exp. Neurol. 240, 146-156.

Ebneter A., Casson R. J, Wood J. P. and Chidlow G. (2010) Microglial activation in the visual pathway in experimental glaucoma: spatiotemporal characterization and correlation with axonal injury. Invest. Ophthalmol. Vis. Sci. 51, 6448-6460.

This article is protected by copyright. All rights reserved.

Accepted Article

Fernandez D. C., Pasquini L. A., Dorfman D., Aldana Marcos H. J. and Rosenstein R. E. (2012) Early distal axonopathy of the visual pathway in experimental diabetes. Am. J. Pathol. 180, 303-313.

Garcia-Valenzuela E., Sharma S. C. and Piña A. L. (2005) Multilayered retinal microglial response to optic nerve transection in rats. Mol. Vis. 11, 225-231.

Guasti L., Richardson D., Jhaveri M., Eldeeb K., Barrett D., Elphick M. R., Alexander, S. P. H., Kendall D., Michael G. J. and Chapman V. (2009) Minocycline treatment inhibits microglial activation and alters spinal levels of endocannabinoids in a rat model of neuropathic pain. Mol. Pain 5, 35.

Hernandez M. R. (2000) The optic nerve head in glaucoma: role of astrocytes in tissue remodeling. Prog. Retin. Eye Res. 19, 297-321.

Howell G. R., Libby R. T., Jakobs T. C., Smith R. S., Phalan F. C., Barter J. W., Barbay J. M., Marchant J. K., Mahesh N., Porciatti V., Whitmore A. V., Masland R. H. and John S.W. (2007) Axons of retinal ganglion cells are insulted in the optic nerve early in DBA/2J glaucoma. J. Cell Biol. 179, 1523-1537.

Ishikawa M., Yoshitomi T., Zorumski C. F. and Izumi Y. (2015) Experimentally Induced Mammalian Models of Glaucoma. Biomed. Res. Int. 2015, 281214.

Jakobs T. C., Libby R. T., Ben Y., John S. W. and Masland, R. H. (2005) Retinal ganglion cell degeneration is topological but not cell type specific in DBA/2J mice. J. Cell Biol. 171, 313-325.

This article is protected by copyright. All rights reserved.

Accepted Article

Kashiwagi K., Ou B., Nakamura S., Tanaka Y., Suzuki M. and Tsukahara S. (2003) Increase in dephosphorylation of the heavy neurofilament subunit in the monkey chronic glaucoma model. Invest. Ophthalmol. Vis. Sci. 44,154-159.

Kerr N. M., Johnson C. S., Green C. R. and Danesh-Meyer H. V. (2011) Gap junction protein connexin43 (GJA1) in the human glaucomatous optic nerve head and retina. J. Clin. Neurosci. 18, 102-108.

Kondo Y., Takada M., Honda Y. and Mizuno N. (1993) Bilateral projections of single retinal ganglion cells to the lateral geniculate nuclei and superior colliculi in the albino rat. Brain Res. 608, 204-215.

Lee J. E., Liang K. J., Fariss R. N. and Wong W. T. (2008) Ex vivo dynamic imaging of retinal microglia using time-lapse confocal microscopy. Invest. Ophthalmol. Vis. Sci. 49, 4169-4176.

Lee W., Moon M., Kim H. G., Lee T. H. and Oh M. S. (2015) Heat stress-induced memory impairment is associated with neuroinflammation in mice. J. Neuroinflammation 12,102.

Leterrier J. F., Kas J., Hartwig J., Vegners R. and Janmey P. A. (1996) Mechanical effects of neurofilament cross-bridges, modulation by phosphorylation, lipids, and interactions with F-actin J. Biol. Chem. 271, 15687-15694.

Levkovitch-Verbin H., Kalev-Landoy M., Habot-Wilner Z., Melamed S. (2006) Minocycline delays death of retinal ganglion cells in experimental glaucoma and after optic nerve transection. Arch. Ophthalmol. 124, 520-526.

This article is protected by copyright. All rights reserved.

Accepted Article

Levkovitch-Verbin H., Waserzoog Y., Vander S., Makarovsky D. and Piven I. (2014) Minocycline upregulates pro-survival genes and downregulates pro-apoptotic genes in experimental glaucoma Graefes Arch. Clin. Exp. Ophthalmol. 252, 761-772.

Libby R. T., Anderson M. G., Pang I. H., Robinson Z. H., Savinova O. V., Cosma I. M., Snow A., Wilson L. A., Smith R. S., Clark A. F. and John S. W. M. (2005) Inherited glaucoma in DBA/2J mice: pertinent disease features for studying the neurodegeneration. Vis. Neurosci. 22, 637-648.

Martin K. R., Quigley H. A., Valenta D., Kielczewski J. and Pease M. E. (2006) Optic nerve dynein motor protein distribution changes with intraocular pressure elevation in a rat model of glaucoma. Exp. Eye Res. 83, 255-262.

Moreno M. C., Marcos H. J., Oscar Croxatto J., Sande P. H., Campanelli J., Jaliffa C. O., Benozzi J. and Rosenstein R. E. (2005) A new experimental model of glaucoma in rats through intracameral injections of hyaluronic acid. Exp. Eye Res. 81, 71-80.

Morrison J. C., Cepurna W. O., Ying Guo. and Johnson E. C. (2011) Pathophysiology of human glaucomatous optic nerve damage: insights from rodent models of glaucoma. Exp. Eye Res. 93, 156-164.

Musch D. C., Gillespie B. W., Lichter P. R., Niziol, L. M. and Janz N. K; CIGTS Study Investigators. (2009) Visual field progression in the Collaborative Initial Glaucoma Treatment Study the impact of treatment and other baseline factors. Ophthalmology 116, 200-207.

This article is protected by copyright. All rights reserved.

Accepted Article

Nakazawa T., Nakazawa C., Matsubara A., Noda K., Hisatomi T., She H., Michaud N., Hafezi-Moghadam A., Miller J. W. and Benowitz L. I. (2006) Tumor necrosis factor-alpha mediates oligodendrocyte death and delayed retinal ganglion cell loss in a mouse model of glaucoma. J. Neurosci. 26,12633-12641.

Naskar R., Wissing M. and Thanos S. (2002) Detection of early neuron degeneration and accompanying microglial responses in the retina of a rat model of glaucoma. Invest. Ophthalmol. Vis. Sci. 43, 2962-2968.

Neufeld A. H. (1999) Microglia in the optic nerve head and the region of parapapillary chorioretinal atrophy in glaucoma. Arch. Ophthalmol. 117, 1050-1056.

Neufeld A. H. and Liu B. (2003) Glaucomatous optic neuropathy: when glia misbehave. Neuroscientist 9, 485-495.

Nixon R. A. and Sihag R. K. (1991) Neurofilament phosphorylation, a new look at regulation and function. Trends Neurosci. 14, 501-506.

Pasquini L. A., Calatayud C. A., Bertone Uña A. L., Millet V., Pasquini J. M. and Soto E. F. (2007) The neurotoxic effect of cuprizone on oligodendrocytes depends on the presence of pro-inflammatory cytokines secreted by microglia. Neurochem. Res. 32, 279-292.

Pease M. E., McKinnon S. J., Quigley H. A., Kerrigan-Baumrind L. A. and Zack D. J. (2000) Obstructed axonal transport of BDNF and its receptor TrkB in experimental glaucoma. Invest. Ophthalmol. Vis. Sci. 41, 764-774.

This article is protected by copyright. All rights reserved.

Accepted Article

Peng B., Xiao J., Wang K., So K. F., Tipoe G. L. and Lin B. (2014) Suppression of microglial activation is neuroprotective in a mouse model of human retinitis pigmentosa. J. Neurosci. 34, 8139-8150.

Perry V. H. and Teeling J. (2013) Microglia and macrophages of the central nervous system: the contribution of microglia priming and systemic inflammation to chronic neurodegeneration. Semin. Immunopathol. 35, 601-612.

Qu J. and Jakobs T. C. (2013) The time course of gene expression during reactive gliosis in the optic nerve. PLoS One 8, e67094.

Quigley HA. (2011) Glaucoma. Lancet 377, 1367-1377.

Quigley H. A., Nickells R. W., Kerrigan L. A., Pease M. E., Thibault D. J. and Zack D.J. (1995) Retinal ganglion cell death in experimental glaucoma and after axotomy occurs by apoptosis. Invest. Ophthalmol. Vis. Sci. 36, 774-786.

Quigley H. A., McKinnon S. J., Zack D. J., Pease M. E., Kerrigan-Baumrind L. A., Kerrigan D. F. and Mitchell R. S. (2000) Retrograde axonal transport of BDNF in retinal ganglion cells is blocked by acute IOP elevation in rats. Invest. Opthalmol. Vis. Sci. 41, 3460-3466.

Raivich G. and Banati R. (2004) Brain microglia and blood-derived macrophages: molecular profiles and functional roles in multiple sclerosis and animal models of autoimmune demyelinating disease. Brain Res. Brain Res. Rev. 46, 261-281.

This article is protected by copyright. All rights reserved.

Accepted Article

Sappington R. M., Carlson B. J., Crish S. D. and Calkins D. J. (2010) The microbead occlusion model: a paradigm for induced ocular hypertension in rats and mice. Invest. Ophthalmol. Vis. Sci. 51, 207-216.

Schlamp C. L., Li Y., Dietz J. A., Janssen K. T. and Nickells R. W. (2006) Progressive ganglion cell loss and optic nerve degeneration in DBA/2J mice is variable and asymmetric. BMC Neurosci. 7, 66.

Sihag R. K., Inagaki M., Yamaguchi T., Shea T. B. and Pant H. C. (2007) Role of phosphorylation on the structural dynamics and function of types III and IV intermediate filaments. Exp. Cell Res. 313, 2098-2109.

Sobrado-Calvo P., Vidal-Sanz M. and Villegas-Perez M. P. (2007) Rat retinal microglial cells under normal conditions, after optic nerve section, and after optic nerve section and intravitreal injection of trophic factors or macrophage inhibitory factor. J. Comp. Neurol. 501, 866-878.

Son J. L., Soto I., Oglesby E., Lopez-Roca T., Pease M. E., Quigley H. A. and Marsh-Armstrong N. (2010) Glaucomatous optic nerve injury involves early astrocyte reactivity and late oligodendrocyte loss. Glia 58, 780-789.

Soto I., Oglesby E., Buckingham B. P., Son J. L., Roberson E. D., Steele M. R., Inman D. M., Vetter M. L., Horner P. J. and Marsh-Armstrong N. (2008) Retinal ganglion cells downregulate gene expression and lose their axons within the optic nerve head in a mouse glaucoma model. J. Neurosci. 28, 548-561.

This article is protected by copyright. All rights reserved.

Accepted Article

Streit W. J., Conde J. R., Fendrick S. E., Flanary B. E. and Mariani C. L. (2005) Role of microglia in the central nervous system's immune response. Neurol. Res. 27, 685-691.

Sun D. and Jakobs T. C. (2012) Structural remodeling of astrocytes in the injured CNS. Neuroscientist 18, 567-88.

Tambuyzer B. R., Ponsaerts P. and Nouwen E. J. (2009) Microglia: gatekeepers of central nervous system immunology. J. Leukoc. Biol. 85, 352-370.

Tan C., Hu T., Peng M. C., Liu S. L., Tong J. B., Ouyang W. and Le Y. (2015) Age of rats seriously affects the degree of retinal damage induced by acute high intraocular pressure. Curr. Eye Res. 40, 300-306.

Wang K., Peng B. and Lin B. (2014) Fractalkine receptor regulates microglial neurotoxicity in an experimental mouse glaucoma model. Glia 62,1943-1954.

Yang M. H., Dibas A. and Tyan Y. C. (2013) Changes in retinal aquaporin-9 (AQP9) expression in glaucoma. Biosci. Rep. 33, e00035.

You Y., Gupta V. K., Graham S. L. and Klistorner A. (2012) Anterograde degeneration along the visual pathway after optic nerve injury. PLoS One 7, e52061.

Yuan L. and Neufeld A. H. (2001) Activated microglia in the human glaucomatous optic nerve head. J. Neurosci. Res. 64, 523-532.

This article is protected by copyright. All rights reserved.

Accepted Article

Zhou X., Li F., Kong L., Chodosh J. and Cao W. (2009) Anti-inflammatory effect of pigment epithelium-derived factor in DBA/2J mice. Mol. Vis. 15, 438-450.

LEGENDS

Figure 1. Immunohistochemical detection of Brn3a in vehicle- and CS-injected eyes. Left panel: Shown are representative photomicrographs of 5 retinas/group. The presence of Brn3a(+) cells was confined to the GCL in all experimental groups. Scale bar = 50 μm. Right panel: Quantification of Brn3a(+) cell number. A significant decrease in this parameter was observed in eyes submitted to ocular hypertension for 10 and 15 (but not 6) weeks. No differences were observed in vehicle-injected eyes between 6, 10, and 15 weeks of treatment. Data are mean ± SEM (n = 5 retinas per group), $^{**}P < 0.01$ vs. vehicle-injected eyes at the same weeks of treatment, by Tukey's test.

Figure 2. CTB tracing studies. Retinal terminal projections in the SC and LGN, and CTB staining in the ON from naïve animals or from animals that were injected with vehicle in one eye and CS in the contralateral eye. Panel A: Photomicrographs showing the CTB-staining pattern in the superficial layers of the SC from an animal whose eyes remained intact, and animals in which one eye was injected with vehicle and the contralateral eye received CS for 3, 6 or 15 weeks. In the SC contralateral to the eye submitted to vehicle injections for 3, 6 or 15 weeks, CTB staining was similar to that found in the SC which received projections from naïve eyes. No differences in CTB staining were observed between SC receiving projections from vehicle- or CS-injected eyes for 3 weeks. In the SC contralateral to an eye with 6 weeks of ocular hypertension, a clear reduction in retinal terminal density was observed, whereas at 15 weeks of ocular hypertension a further decrease in CTB staining and zones of no staining were found. Scale bar = 2 mm. Panel B: Photomicrographs showing CTB-staining in the LGN. Ocular hypertension for 6 or 15 (but not 3) weeks induced a decrease in CTB staining in the LGN. Scale bar = 200 μm. Panel C: Representative CTB staining in longitudinal

This article is protected by copyright. All rights reserved.

Accepted Article

section of ON proximal portion from eyes injected with vehicle or CS for 6 weeks. Ocular hypertension induced and arrest of CTB transport at a myelinated portion (beyond the ONH), as shown by MBP immunoreactivity distribution in a control ON (upper image). Scale bar = 0.15 mm. Shown are representative images of five animals per group.

Figure 3. pNFH-immunoreactivity. Left panel: Representative photomicrographs showing pNFH immunostaining in transverse sections of the proximal portion of the ON from eyes injected with vehicle or CS for 6 or 15 weeks. Detailed images are shown in squared panels. Scale bar = 100 µm. Right panel: Quantification of the pNFH(+) area in the proximal ON. Ocular hypertension induced a significant decrease in this parameter at both time points. Data are mean ± SEM (n = 5 ONs per group), $^{**}P < 0.01$ vs. vehicle-injected eyes at the same week of treatment, by Tukey's test.

Figure 4. Microglia analysis in the proximal ON portion. Panel A: Representative photomicrographs showing Iba-1- (upper panel), and ED1 (lower panel)-immunostaining patterns in cross-sections of ONs from eyes injected with vehicle or CS for 6 and 15 weeks. Scale bar = 100 µm. Detailed images are shown in squared panels. Panel B: Analysis of Iba-1(+) and ED1(+) area. At 6 weeks of ocular hypertension, a significant increase of Iba-1(+) area which was lower than that observed at 15 weeks of treatment with CS was observed. ED1 immunoreactivity was undetectable in vehicle-injected eyes for 6 or 15 weeks, whereas CS injections induced a significant increase in this parameter at 6 weeks, which was higher at 15 weeks. Data are the mean ± SEM (n = 5 ONs per group); $^{**}P < 0.01$, vs. vehicle-injected eyes, a: $P < 0.01$ vs. eyes injected with CS for 6 weeks, by Tukey's test.

Figure 5. Analysis of GFAP-immunoreactivity and myelination in the proximal portion of the ON. Panel A: Representative photomicrographs showing GFAP-immunoreactivity in cross-sections from ONs at 6 or 15 weeks of vehicle or CS intracameral injections. Scale bar = 100 µm. Panel B:

This article is protected by copyright. All rights reserved.

Accepted Article

Representative cross-sections of proximal portion of the ON from eyes injected with vehicle or CS for 6 and 15 weeks stained with LFB. Scale bar = 50 µm. A compact myelin staining was observed in ONs from vehicle-injected eyes at both time points. Note a lessened stain intensity in ONs from eyes injected with CS for 6 and 15 weeks. Panel C: Quantification of GFAP-immunoreactivity and intensity of LFB staining. Ocular hypertension induced a significant increase in GFAP(+) area and a decrease in LFB staining at both time points. Data are mean ± SEM (n = 5 ONs per group). $^{**}P < 0.01$ vs. vehicle-injected eyes, a: $P < 0.01$ vs. CS-injected eyes for 6 weeks, by Tukey's test.

Figure 6. Effect of minocycline on ON microglia. Panel A: Representative photomicrographs showing Iba1- and ED1-immunoreactivity in ONs from eyes injected with vehicle or CS for 6 weeks from animals treated with saline solution (SS) or minocycline (MINO). SS or MINO were daily injected (30 mg/kg, i.p.) for 2 weeks, starting at 4 weeks of treatment with vehicle or CS. Scale bar = 100 µm. Panel B: Analysis of Iba-1(+) and ED1(+) area. Minocycline, which showed no effect in ONs from vehicle-injected eyes, significantly decreased these parameters in ONs from hypertensive eyes. Data are mean ± SEM (n = 5 ONs per group). $^{**}P < 0.01$ vs. vehicle-injected eyes from animals treated with SS, a: $P < 0.01$ vs. hypertensive eyes from animals injected with SS, by Tukey's test.

Figure 7. Effect of minocycline on GFAP-immunoreactivity and LFB staining in the proximal ON. Panel A: Representative photomicrographs showing GFAP-immunoreactivity in ON transverse sections from eyes injected with vehicle or CS. Scale bar = 100 µm. Panel B: Representative photomicrographs of ONs stained with LFB. Scale bar = 25 µm. Panel C: Quantification of GFAP-immunoreactivity and intensity of LFB staining. Minocycline, significantly prevented the increase in GFAP(+) area and the decrease in LFB staining induced by ocular hypertension. Data are mean ± SEM (n = 5 ONs per group). $^{**}P < 0.01$ vs. vehicle-injected eyes from animals treated with SS, a: $P < 0.01$ and b: $P < 0.05$ vs. CS-injected eyes from animals injected with SS, by Tukey's test.

This article is protected by copyright. All rights reserved.

Accepted Article

Figure 8. Effect of minocycline on pNFH-immunolabeling and CTB anterograde transport. Panel A (left): Representative photomicrographs showing pNFH-immunoreactivity in transverse sections of the proximal portion of the ON from animals treated with SS or MINO. Scale bar = 100 µm. Panel A (right): Quantification of pNFH(+) area in the ON. Minocycline significantly prevented the decrease pNFH-immunoreactivity induced by ocular hypertension. In vehicle-injected eyes, pNFH-immunoreactivity did not differ between SS- and minocycline-treated animals. Data are mean ± SEM (n = 5 ONs per group). **P <0.01 vs. vehicle-injected eyes from animals treated with SS, a: $P < 0.01$ vs. CS-injected eyes from animals treated with SS, by Tukey's test. Panel B: CTB anterograde transport to the SC (right; scale bar = 2 mm) and LGN (left; scale bar = 200 µm) representative from 5 animals per group. Minocycline prevented the decrease in CTB transport from the retina to both projections areas induced by ocular hypertension.

This article is protected by copyright. All rights reserved.

Table I. IOP values of rats injected with vehicle in one eye and CS in the contralateral eye for 3, 6, 10 or 15 weeks

IOP values (mm Hg)

Treatment length	Vehicle	CS
3 weeks	13.6 ± 0.5	22.3 ± 0.9**
6 weeks	12.5 ± 0.7	21.3 ± 0.7**
10 weeks	12.3 ± 0.6	22.9 ± 1.0**
15 weeks	13.2 ± 0.6	23.2 ± 1.0**

IOP was assessed with a Tonopen XL in rats injected with CS in one eye and vehicle in the contralateral eye for 3, 6, 10 or 15 weeks. At all these intervals, CS injections induced a significant increase in this parameter. No differences were observed in control eyes among 3, 6, 10 and 15 weeks of treatment (ANOVA). Data are mean ± SE (n = 20 eyes/group) **$P < 0.01$, by Student's test.

Accepted Article

This article is protected by copyright. All rights reserved.

Accepted Article

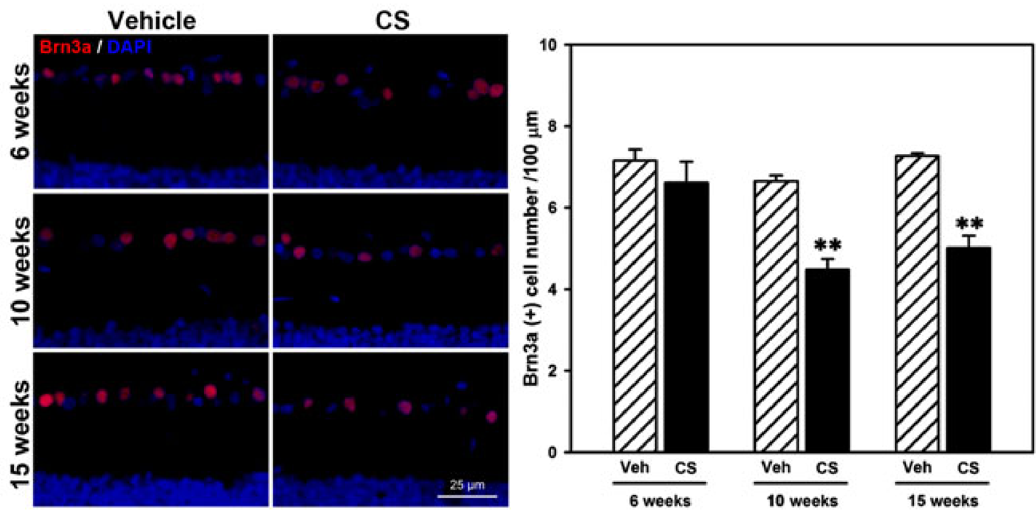

A
Intact
3 weeks
6 weeks
15weeks
Veh CS
Veh CS
Veh CS
C
CTB/MBP
vehicle
CTB
vehicle
CS
B
Intact
3 weeks
6 weeks
15 weeks
veh CS
veh CS
veh CS
dLGN
IGL
vLGN

This article is protected by copyright. All rights reserved.

Accepted Article

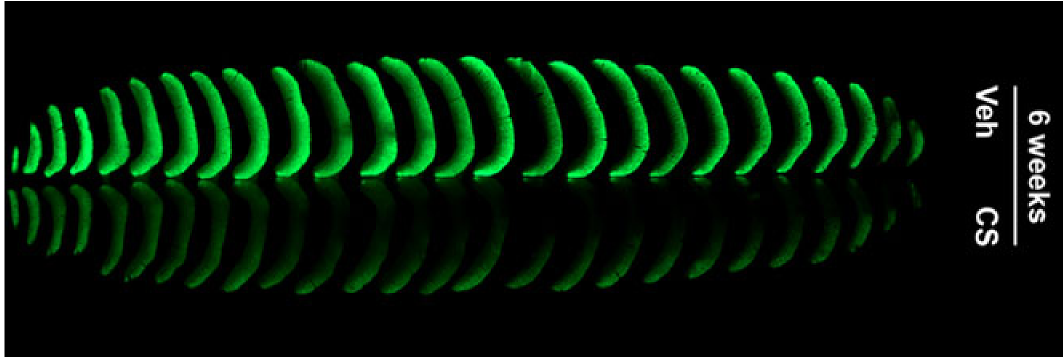

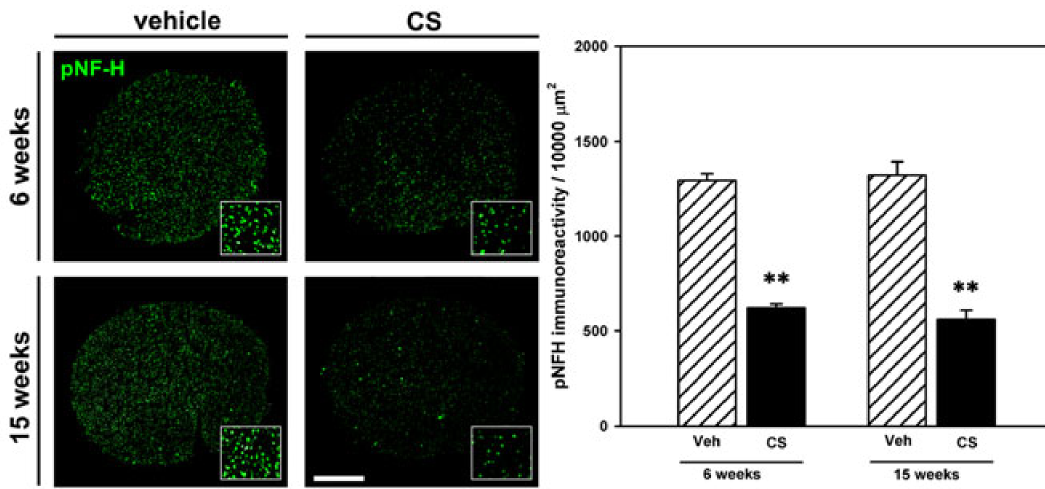

This article is protected by copyright. All rights reserved.

Accepted Article

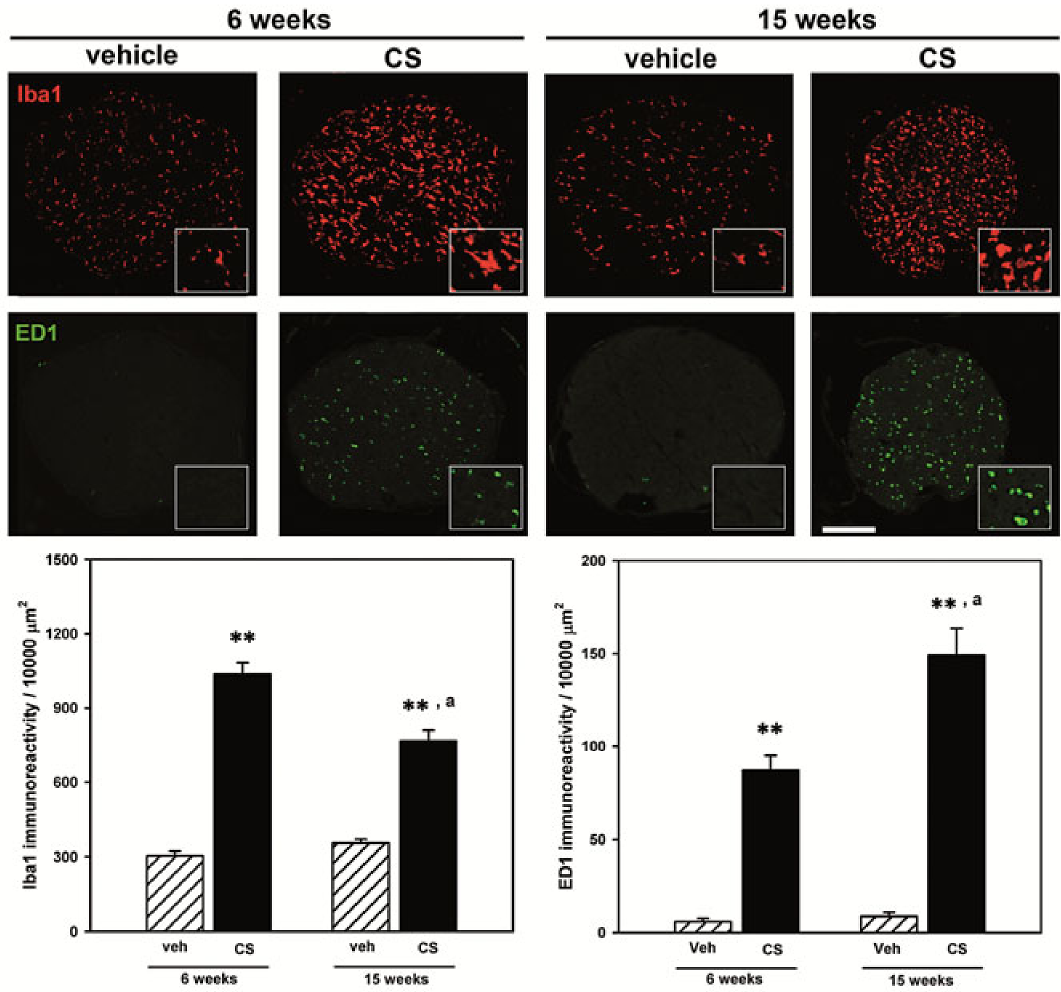

This article is protected by copyright. All rights reserved.

Accepted Article

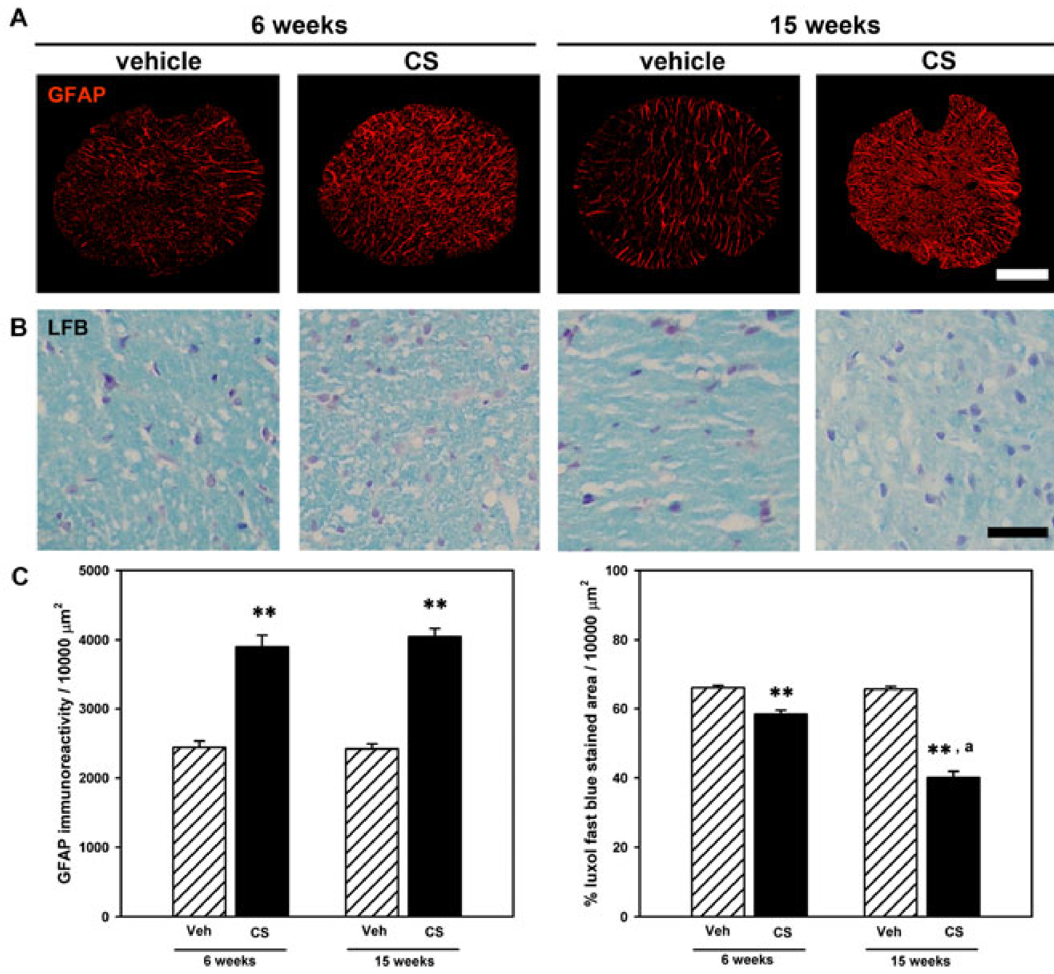

This article is protected by copyright. All rights reserved.

Accepted Article

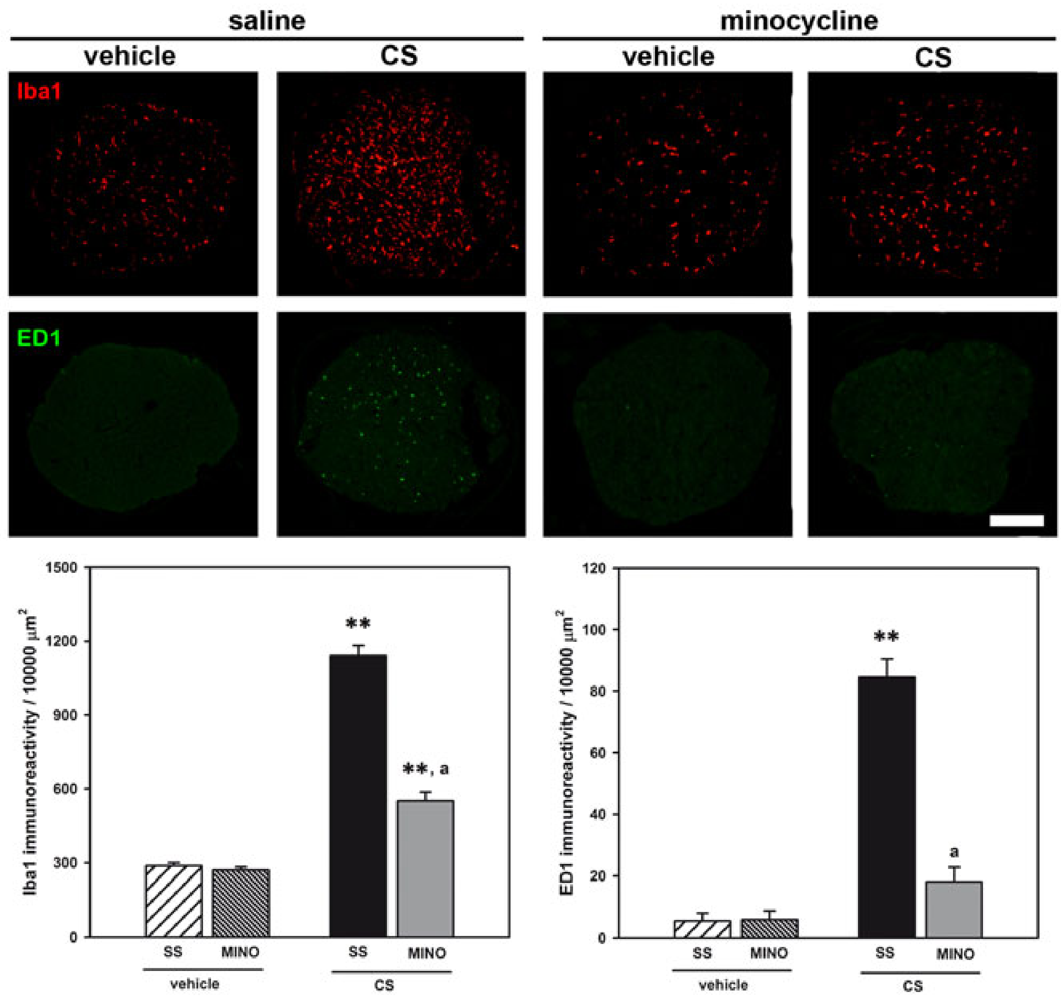

This article is protected by copyright. All rights reserved.

Accepted Article

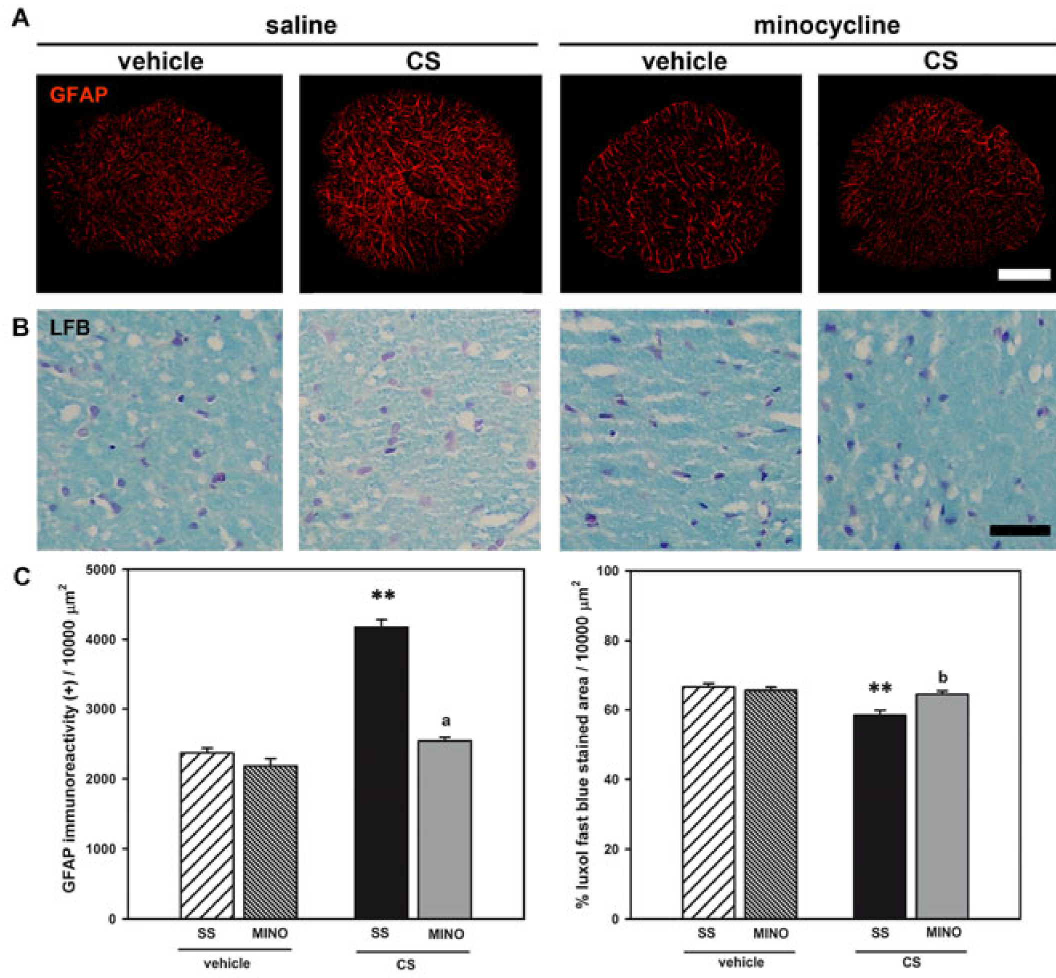

This article is protected by copyright. All rights reserved.

Accepted Article

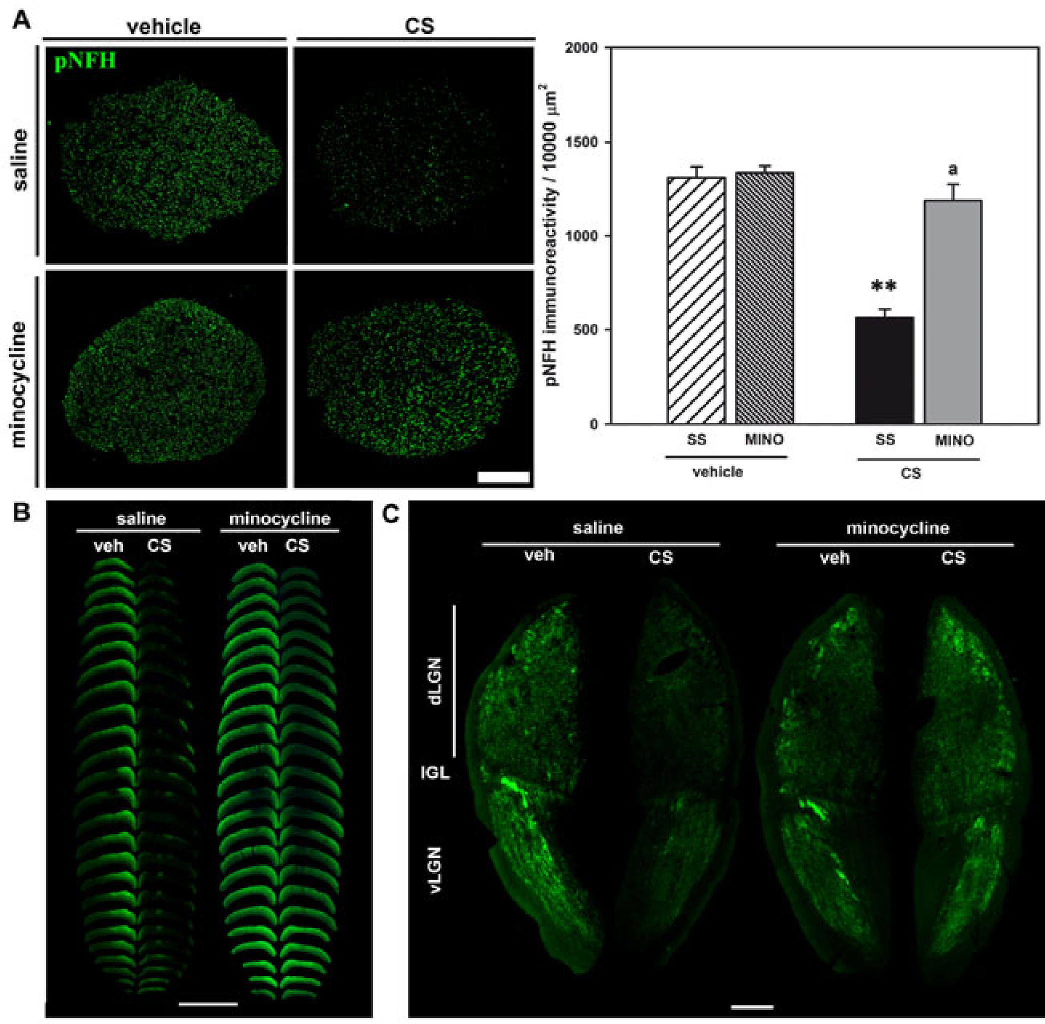

This article is protected by copyright. All rights reserved.